A Comprehensive Analysis Of Different Density Distributions Of Neutron-Rich ^{14}Be Exotic Nucleus

Murat AYGÜN [1],♠

[1]*Bitlis Eren University, Faculty of Arts and Sciences, Department of Physics, Bitlis, Turkey,*

ABSTRACT

The quasielastic scattering angular distribution of the ^{14}Be projectile scattered from the ^{12}C target nucleus at incident energy of 796 MeV is analyzed by using the double folding model. In this context, the eight different density distributions of ^{14}Be are used to obtain the real part of the optical potential. The imaginary potentials of all the density distributions are taken as Woods-Saxon type. The theoretical results obtained for each density distribution are compared with each other as well as the experimental data. These comparisons provide information about the similarities and differences of the density distributions used in the theoretical analysis.

Keywords: Optical model, Double folding model, Elastic scattering.

1. INTRODUCTION

The experimental and theoretical studies conducted in the field of nuclear physics have provided a very important contribution to our understanding of the properties of the nucleus. These studies have often been conducted with nuclei located in the stability region. Therefore, sufficient information on unstable nuclei could not be obtained. In the last few decades, as a result of technological progress, the scope of studies performed in the field of nuclear physics has expanded. Thus, it has become more possible to study the subjects that have not been sufficiently known. Some unstable nuclei from the experimental and theoretical studies performed for this purpose have been noticed to show

very important structural differences such as large matter radius, extremely small two-neutron separation energy (S_{2n}), weakly bound valence nucleons, the large reaction cross-sections, the change of magic numbers as compared to the stable nuclei [1-6]. Such nuclei are referred to as halo nuclei. At the present time, halo nuclei still continue to be one of the most important subject in the field of nuclear physics [7-15]. The ^{14}Be nucleus, a secondary beam produced with bombardment of a thick target such as Be [16], is a neutron halo nucleus which has anomalously large matter radii [17]. ^{14}Be whose the two-neutron separation energy is known to be 1.34 ± 0.1 MeV [18] is also a Borromean nucleus where the system is bound. ^{14}Be has often been

♠Corresponding author, e-mail: *murata.25@gmail.com*

assumed to be described as a three-body system composed by ^{12}Be+n+n. In addition to this, the ^{14}Be nucleus has been considered as five-body system with ^{10}Be+n+n+n+n [19]. The ^{14}Be nucleus has attracted much interest due to its neutron-rich structure, and many experimental and theoretical studies have been performed [19-22]. The density distributions of stable nuclei have been intensively studied by electron scattering and by proton scattering. For these nuclei, the experimental data can be described via a Woods-Saxon type density distribution or a Fermi type density distribution or a harmonic-oscillator type density distribution [23,24]. On the other hand, the density distribution of halo nuclei presents a long tail in loosely bound nucleus close to the neutron or proton drip lines. Also, the cross-section of nucleus-nucleus scattering is sensitive to the density distribution [25,26]. Henceforth, it is important to examine the density distributions of halo nuclei. Various density distributions for the ^{14}Be nucleus can be found in the literature [27]. These are the Single-Gaussian (SG), Gaussian-Gaussian (GG), Gaussian-Halo (GH), Gaussian-Oscillator (GO), Fermi-Gaussian (FG) and Gaussian-Exponential (GE) density distributions. In this context, a comparative analysis of these different density profiles probed by reactions with ^{14}Be can be useful. A measurement of quasielastic scattering of the ^{14}Be + ^{12}C system for 796 MeV at Michigan State University was performed by Zahar et al. [28]. They carried out the phenomenological calculations within the optical model (OM) and inelastic scattering for the 2^+ excited state of the ^{12}C nucleus in the coupled-channels (CC) formalism in order to explain the experimental data. They showed that the ^{14}Be + ^{12}C system needs a potential with a much deeper surface imaginary component and an attractive surface real component to obtain a good agreement with the experimental data. The other theoretical analysis of quasielastic scattering of the ^{14}Be + ^{12}C system at incident energy of 796 MeV was performed by Mermaz [29]. With this goal, Mermaz conducted the OM calculations with volume Woods-Saxon (WS) type plus surface terms for the real and imaginary potentials. Although they generally used the phenomenological approach within the framework of the OM, a microscopic approach such as double folding model (DFM) was not applied to the analysis of this reaction. The DFM together the density distributions of both projectile nucleus and target nucleus [30] can be used in order to obtain the real part of the optical potential. In the present study, we focus on the analysis of the ^{14}Be + ^{12}C system for eight different density distributions of the ^{14}Be nucleus by using the DFM based on the OM. We obtain the angular distributions of the scattering data for all the density distributions. Then, the cross-sections obtained for each density distribution are compared with results of the previous studies as well as the experimental data. This comparison between the cross-sections obtained with several shapes of the matter density distribution from the theoretical analysis [31] suggests how to select among the different density profiles. In the next section, we present the OM calculations. In section 3, we define all the density distributions handled in the present study. In Section 4,

the results of these calculations are presented. Section 5 is devoted to our summary and conclusion.

2. OPTICAL MODEL CALCULATIONS

Here, we briefly outline the method conducted in the theoretical analysis of the quasielastic scattering data of the ^{14}Be + ^{12}C system within the framework of the OM. The nuclear potential has the real and imaginary parts. In determining the real part of nuclear potential, the DFM is used extensively. To achieve the double folding potential, the nuclear matter distributions of both projectile nucleus and target nucleus together with an effective nucleon-nucleon interaction potential (v_{NN}) are evaluated. Thus, the double folding potential is

$$V_{DF}(r) = \int dr_1 \int dr_2 \rho_P(r_1)\rho_T(r_2)v_{NN}(r_{12}) \qquad (1)$$

where $\rho_P(r_1)$ and $\rho_T(r_2)$ are the nuclear matter densities of projectile and target nuclei, respectively. In our calculations, the eight different density distributions of ^{14}Be have been used to make a comparative study. Each of these density distributions is explained in the following section. However, the density distribution of the ^{12}C target nucleus is taken as

$$\rho_{^{12}C}(r_2) = \rho_0(1 + wr_2^2)\exp(-\beta r_2^2) \qquad (2)$$

where ρ_0=0.1644 fm^{-3}, w=0.4988 fm^{-2}, and β=0.3741 fm^{-2} [32,33]. For the v_{NN} interaction, we have used the M3Y nucleon-nucleon (Michigan 3 Yukawa) realistic interaction [34], which is given by

$$v_{NN}(r) = 7999\frac{\exp(-4r)}{4r} - 2134\frac{\exp(-2.5r)}{2.5r} + J_{00}(E)\delta(r)\, MeV$$
$$(3)$$

where $J_{00}(E)$ is the exchange term in the following form

$$J_{00}(E) = 276\,[1 - 0.005\, E\,/\, A_p]\, MeV\, fm^3 \qquad (4)$$

The imaginary potential of the OM has been taken in the WS type

$$W(r) = -\frac{W_0}{1 + \exp((r - R_w)/a_w)} \qquad (5)$$

where $R_w = r_w(A_P^{1/3} + A_T^{1/3})$. A_P and A_T are mass numbers of the projectile and target nuclei respectively. The code FRESCO [35] has been used for all the calculations.

3. PARAMETRIZATION OF THE DENSITY DISTRIBUTIONS

In our work, we have used the eight different density distributions of ^{14}Be in order to obtain the scattering cross-section of ^{14}Be by ^{12}C. These density distributions are the SG, GG-2n, GG-4n, GH, GO-2n, GO-4n, FG

and GE density distributions, which have free parameters to generate the matter density of [14]Be.

3.1. The Single-Gaussian (SG) density distribution

The nucleon density of the nucleus examined by means of the SG density distribution is calculated by using the following equation [36]

$$\rho(r) = \left(\frac{3}{2\pi R_m^2}\right)^{3/2} \exp\left(-\frac{3r^2}{2R_m^2}\right) \qquad (6)$$

where R_m is the root mean square (rms) matter radius of the nucleus. In our calculations, the value of R_m is 2.96 fm [27].

3.2. The Gaussian-Gaussian (GG) density distribution

The core and halo density distributions of this nucleus for this model has the following Gaussian profiles [37]

$$\rho_c(r) = \left(\frac{3}{2\pi R_c^2}\right)^{3/2} \exp\left(-\frac{3r^2}{2R_c^2}\right) \qquad (7)$$

$$\rho_h(r) = \left(\frac{3}{2\pi R_h^2}\right)^{3/2} \exp\left(-\frac{3r^2}{2R_h^2}\right) \qquad (8)$$

where R_c and R_h are the rms radii of the core and halo nucleon distributions, respectively. The total matter distribution ρ_m is given in following form

$$\rho_m(r) = \left[N_c\rho_c(r) + (A - N_c)\rho_h(r)\right]/A \qquad (9)$$

where N_c and A are the number of nucleons in the core and mass number, respectively. In the present work, we have assumed that [14]Be consists of two different structures as 2n-halo nucleus (GG-2n) and 4n-halo (GG-4n) nucleus. Firstly, the Gaussian density distribution for both [12]Be and 2n has been used. The values of R_c and R_h are taken as 2.79 fm and 5.67 fm, respectively [27]. For these values, we obtained R_m=3.35 fm. Secondly, the Gaussian density distribution for [10]Be and 4n has been used. In this case, the values of R_c and R_h are taken as 2.61 fm and 4.48 fm, respectively [27]. For these values, the value of R_m has been found as 3.25 fm.

3.3. The Gaussian-Halo (GH) density distribution

Another density distribution of [14]Be nucleus is the GH density distribution. The GH density distribution is given by

$$\rho_m(r) = \left(\frac{3}{2\pi R_m^2}\right)^{3/2} \left[1 + \alpha\varphi(r)\right]\exp\left(-\frac{3r^2}{2R_m^2}\right), \qquad (10)$$

where

$$\varphi(r) = \frac{3}{4}\left[5 - 10\left(\frac{r}{R_m}\right)^2 + 3\left(\frac{r}{R_m}\right)^4\right]. \qquad (11)$$

α is a parameter in the range $0 \le \alpha \le 0.4$. For α=0, the GH density distribution has a Gaussian form, whereas for values of α close to 0.4 the density distribution has halo component tail. In our calculations, the values of R_m and α are taken as 3.19 fm and 0.11 fm, respectively [27]. For these values, the rms matter radius of the nucleus is 3.18 fm.

3.4. The Gaussian-Oscillator (GO) density distribution

Here, we assume that the density distribution of the [14]Be nucleus is the sum of the core and the halo density distributions. With this goal, the core density distribution is taken in the following Gaussian form

$$\rho_c(r) = \left(\frac{3}{2\pi R_c^2}\right)^{3/2} \exp\left(-\frac{3r^2}{2R_c^2}\right). \qquad (12)$$

The 1p-shell harmonic oscillator density distribution for the halo density distribution is assumed. This density distribution is given by

$$\rho_h(r) = \frac{5}{3}\left(\frac{5}{2\pi R_h^2}\right)^{3/2}\left(\frac{r}{R_h}\right)^2 \exp\left(-\frac{5r^2}{2R_h^2}\right). \qquad (13)$$

The ρ_m is given in following form

$$\rho_m(r) = \left[N_c\rho_c(r) + (A - N_c)\rho_h(r)\right]/A \qquad (14)$$

In the present study, [14]Be has two different structures such as 2n-halo nucleus (GO-2n) and 4n-halo (GO-4n) nucleus. Firstly, the Gaussian density distribution for [12]Be and the oscillator density distribution for 2n have been used. The values of R_c and R_h are taken as 2.74 fm and 5.50 fm, respectively [27]. We have obtained the value of R_m as 3.09 fm. Then, the Gaussian density distribution for [10]Be and the oscillator density distribution for 4n have been used. The values of R_c and R_h are taken as 2.48 fm and 4.48 fm, respectively [27]. For these values, R_m is 2.97 fm.

3.5. The Fermi-Gaussian (FG) density distribution

This model for [14]Be consists in a core plus a 4n halo. In this context, the density distribution of [14]Be can be taken in the following form

$$\rho_{14_{Be}}(r) = \rho_{10_{Be}}(r) + 4\rho_n(r). \qquad (15)$$

The density distribution of [10]Be is in the Fermi form [38]

$$\rho_{10_{Be}}(r) = \frac{\rho_0}{\left[1 + \exp\left(\frac{r - 2.0}{0.511}\right)\right]}, \qquad (16)$$

where ρ_0 is determined by using the normalization condition

$$4\pi \int \rho(r)r^2 dr = A, \tag{17}$$

where A is mass number of ^{10}Be core. Finally, the density distribution of 1n-halo is in Gaussian form [39,40]

$$\rho_n(r) = \left(\frac{1}{\gamma\sqrt{\pi}}\right)^3 \exp\left(-\frac{r^2}{\gamma^2}\right), \tag{18}$$

where γ is adjusted to reproduce the experimental value for the rms radius of ^{14}Be. For these values, R_m is 3.18 fm.

3.6. The Gaussian-Exponential (GE) density distribution

Here, the density distribution of ^{14}Be is the sum of the core and halo density distributions. The core density distribution is taken in the following Gaussian form

$$\rho_c(r) = \left(\frac{3}{2\pi R_c^2}\right)^{3/2} \exp\left(-\frac{3r^2}{2R_c^2}\right). \tag{19}$$

The exponential density distribution of the halo is given by

$$\rho_h(r) = \left(\frac{r^2}{R_h^5}\right)\exp\left(-\sqrt{30}\,\frac{r}{R_h}\right). \tag{20}$$

In our calculations, the values of R_c and R_h are taken as 2.67 fm and 5.70 fm, respectively [36]. For these values, we obtained R_m=2.71 fm.

4. RESULTS AND DISCUSSIONS

We have conducted the theoretical analysis of quasielastic scattering of the ^{14}Be + ^{12}C system at 796 MeV. For this, we have obtained the eight different density distributions of the ^{14}Be nucleus. All the density distributions have been shown in Figs. 1 (logarithmic scale) and 2 (linear scale) in order to make a comparative work. We have observed that the FG density distribution extends much farther than the other density distributions. However, the GG-4n density distribution is very close to the FG density distribution. The GG-2n and GE density distributions, very similar to each other, extend much farther than the other density distributions except for the FG and GG-4n density distributions. The GH and GO-2n density distributions are essentially identical. The SG density distribution has the shortest tail among the density distributions.
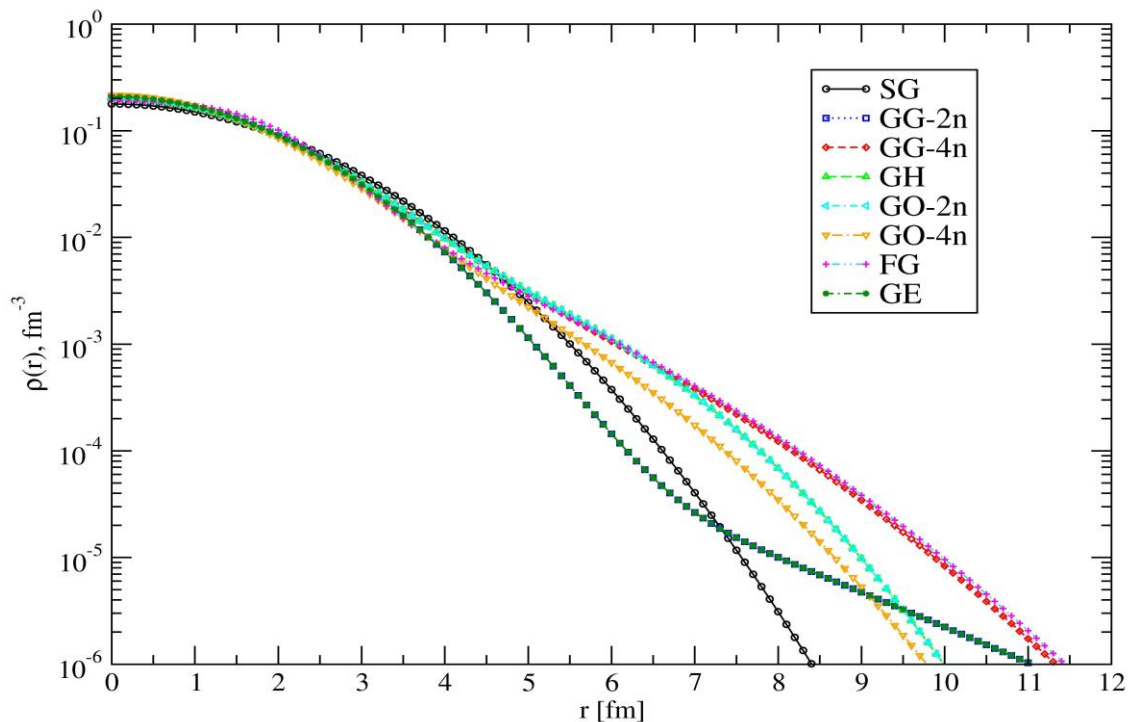

Figure 1. The density distributions of the SG, GG-2n, GG-4n, GH, GO-2n, GO-4n, FG, GE in logarithmic scale.
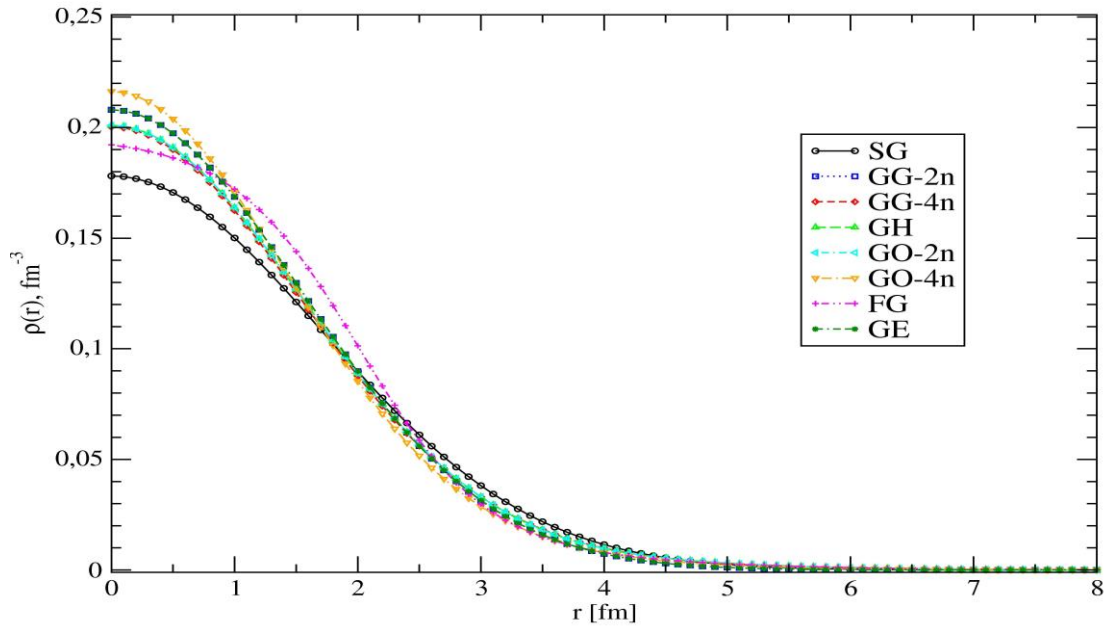
Figure 2. Same as Fig. 1, but in linear scale.

The optical model calculations, with these different density distributions used to define the real part of the optical potential in the DFM, were carried out by searching the parameters W_0, r_w and a_w of the imaginary part of the potential in order to fit the experimental data. Firstly, we have tested different values of r_w in steps from 0.1 to 0.01 fm. After that, the value of r_w=0.99 fm has been fixed for all calculations. Then, we have conducted similar calculations for the value a_w of the imaginary potential in steps of 0.1 and 0.01 fm at fixed radius. Thus, the value of a_w has been fixed to 0.98 fm in the calculations of all the density distributions. The fitting procedure for the studied systems has been completed by adjusting the depth of imaginary potential. The obtained optical potential parameters are listed in Table 1.

Table 1: The microscopic optical potential parameters for the SG, GG-2n, GG-4n, GH, GO-2n, GO-4n, FG, GE density distributions used in the analysis of the ^{14}Be + ^{12}C system at E_{Lab}=796 MeV.

Density distribution	N_R	W (MeV)	r_w (fm)	a_w (fm)	σ(mb)	χ^2/N
SG	0.900	46.50	0.99	0.98	1756.7	4.25
GG-2n	0.900	43.20	0.99	0.98	1721.5	4.25
GG-4n	0.840	40.80	0.99	0.98	1691.8	4.48
GH	0.813	39.50	0.99	0.98	1674.9	4.95
GO-2n	1.000	48.60	0.99	0.98	1781.1	3.76
GO-4n	1.000	47.60	0.99	0.98	1769.9	3.88
FG	1.000	46.00	0.99	0.98	1754.2	3.82
GE	1.100	50.00	0.99	0.98	1793.4	5.78

In Fig. 3, we have presented the theoretical results obtained for each of the density distributions. The SG density distribution appears to represent the experimental data to some extend. The GG-2n and GG-4n density distributions show a behavior very similar to each other. The GO-2n, GO-4n and FG density distributions present a similar behavior and are in good agreement with the experimental data. On the other hand, the GO-2n density distribution is slightly better than the GO-4n and FG density distributions. Also,

when we search for the best fit of the data, we have observed that the results of the GO-2n density distribution are better than the ones obtained with other density distributions. We think that the neutron halo tail is important in explaining the experimental data. In addition to this, density distribution selected for both core and neutron halo is important. Finally, we should say that in general these density distributions reproduced the experimental data.
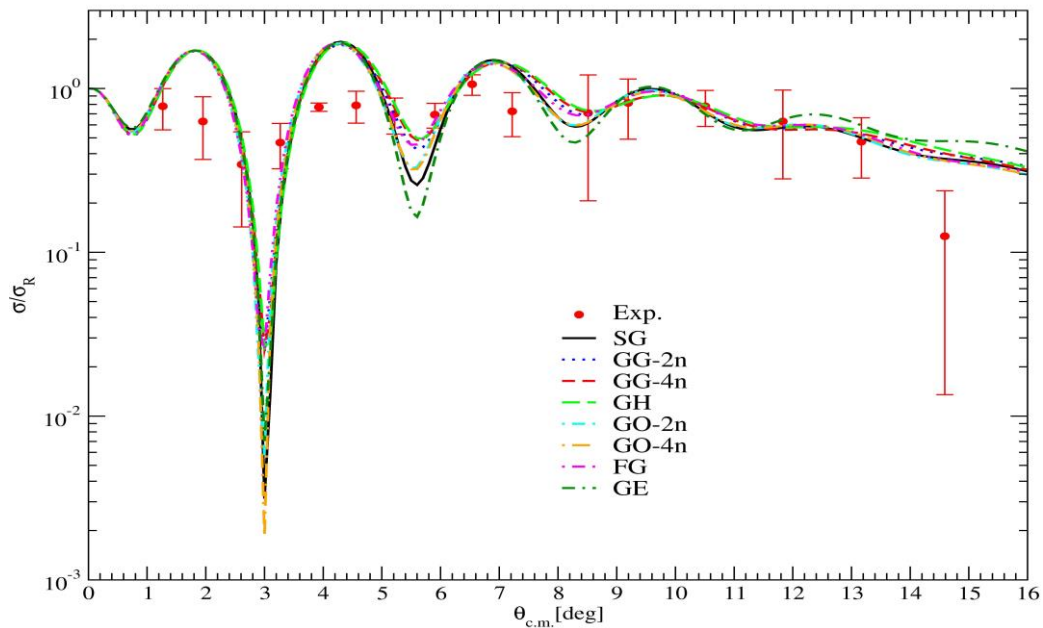

Figure 3. The elastic scattering angular distributions for the SG, GG-2n, GG-4n, GH, GO-2n, GO-4n, FG, GE density distributions of the ^{14}Be + ^{12}C reaction at E_{Lab}=796 MeV in comparison with the experimental data. The experimental data have been taken from [28].
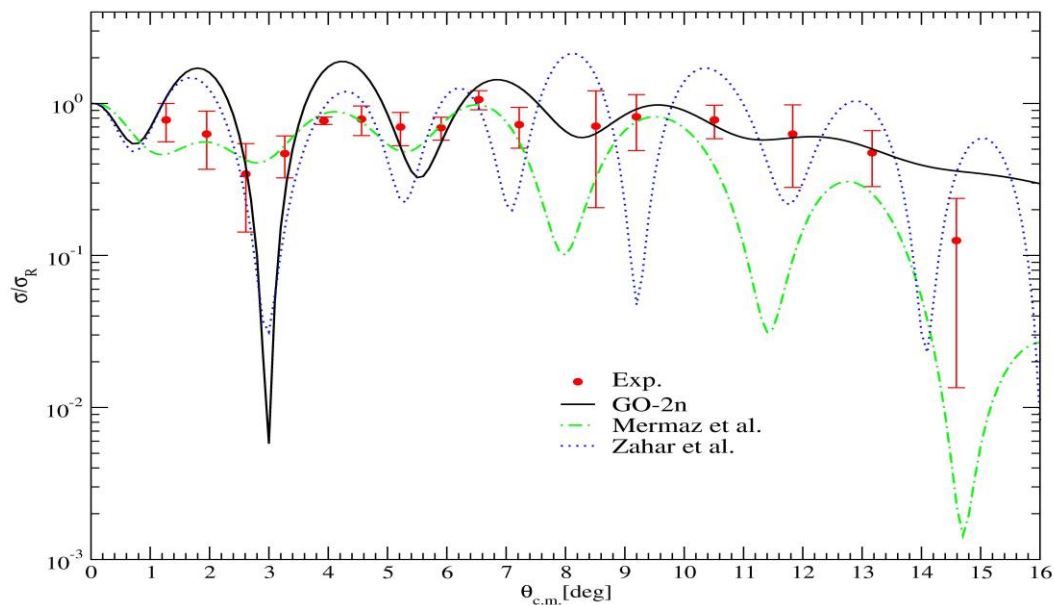

Figure 4. The elastic scattering angular distribution of the GO-2n density distribution in comparison with the previous studies [28,29] as well as the experimental data. The experimental data have been taken from [28].

In Fig. 4, we compared the theoretical results of the GO-2n density distribution which give good agreement results with the experimental data in order to make a comparison work with the previous studies [28,29]. While the results [28,29] have been achieved, we have performed only the phenomenological calculations for the OM parameters given in Refs. [28,29] without including the inelastic scattering of the ^{12}C nucleus. In Refs. [28,29], the theoretical results consist of the sum of the elastic and inelastic scattering. Therefore, we should point out that there is some difference between our results and the results of Refs. [28,29]. However, we have observed that our results are better than the results of previous studies although we have not included the surface potential for both the real and imaginary potentials in our calculations. We deduce that the DFM results with the different density distributions are better than the phenomenological OM results. As a result of this, we think that the internal dynamics of the ^{14}Be exotic nucleus is taken into account by using different density distributions and the DFM.
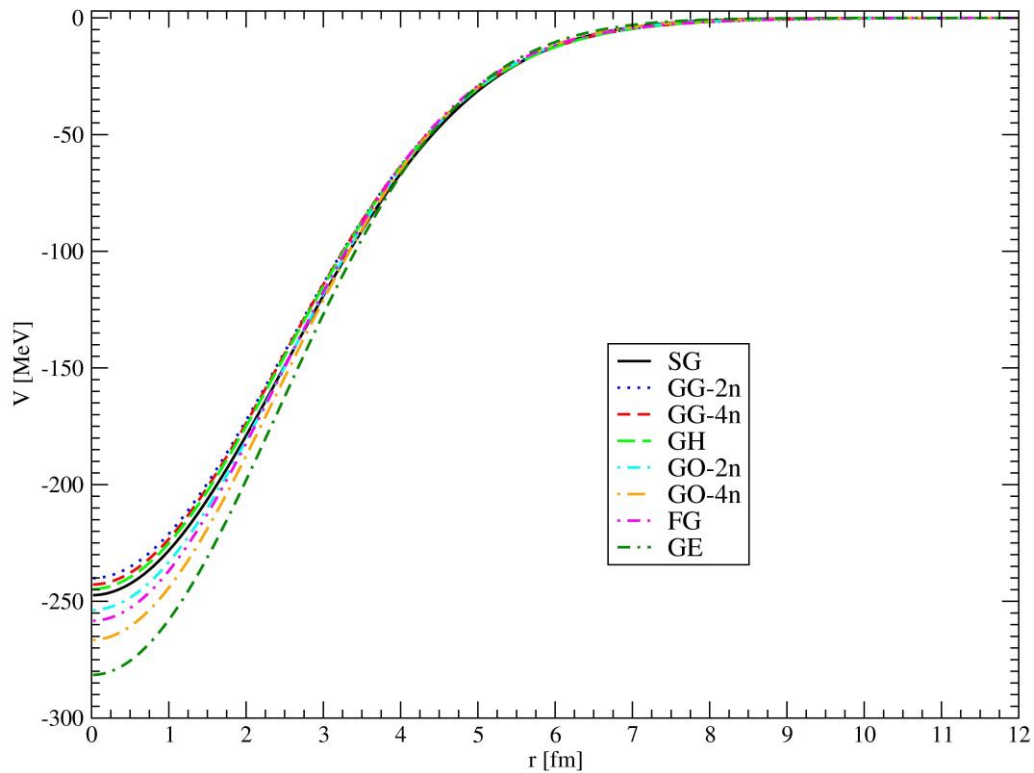

Figure 5. The shapes of the real potentials of the nuclear potential of the ^{14}Be + ^{12}C reaction for the SG, GG-2n, GG-4n, GH, GO-2n, GO-4n, FG, GE density distributions.

In Figs. 5 and 6, the shapes of the real and imaginary potentials used in the theoretical calculations conducted with different density distributions of the ^{14}Be projectile are shown. It has been observed that the real potential of GE density distribution is deeper than the real potentials of the other density distributions. However, the shallow real potential is attributed to the GG-2n density distribution. In case of the imaginary potential, the deepest imaginary potential is found for the GE density distribution and the shallow imaginary potential is observed for the GH density distribution.
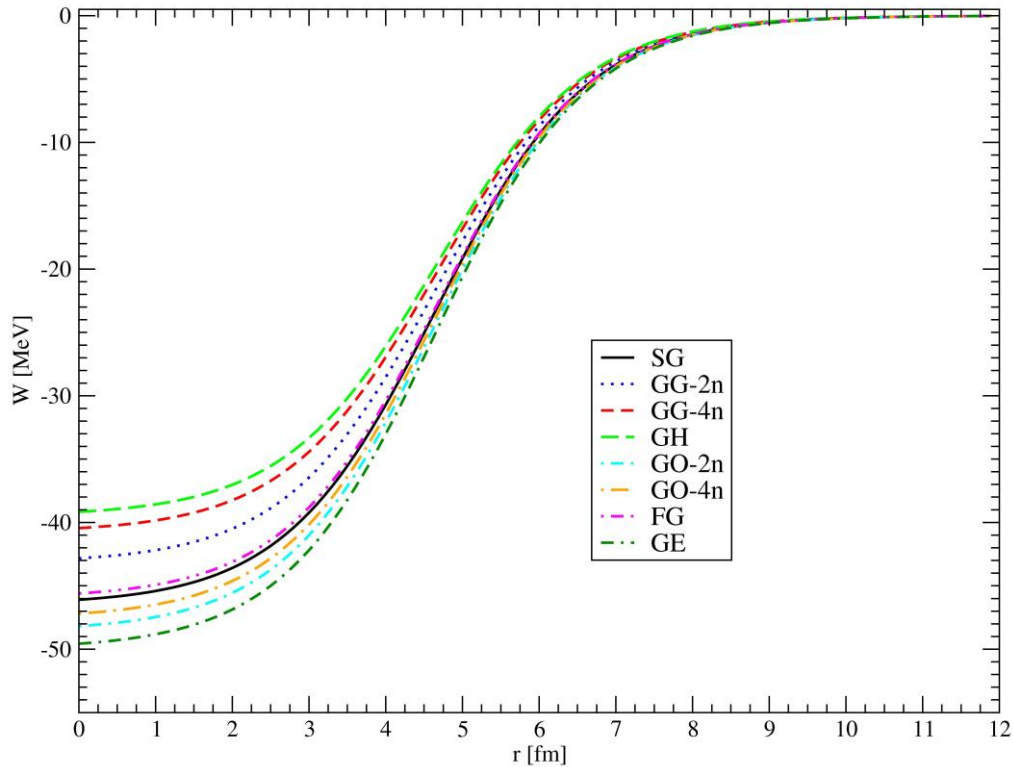
Figure 6. The shapes of the imaginary potentials of the nuclear potential of the ^{14}Be + ^{12}C reaction for the SG, GG-2n, GG-4n, GH, GO-2n, GO-4n, FG, GE density distributions.

We have given the cross-sections of all the density distributions investigated in Table 1. We have noticed that the cross-sections vary in the range of $1674.9 \leq \sigma \leq 1793.4$ mb. Then, we compare our results with the cross-sections of the previous studies. Zahar [28] reported as 1900 mb the value of the cross-section for the ^{14}Be + ^{12}C system. This result is close to the cross-section determined with our study.

In Table 1, we have given the calculated χ^2/N values for each density distribution according to the experimental error around 10%. In this context, if we compare the χ^2/N values of the density distributions, we can see that the GO-2n density has lower χ^2/N value than the other density distributions. On the other hand, the biggest χ^2/N value is found for the GE density distribution.

The normalization (N_R) constant is used to generate good agreement results between the theoretical results and the experimental data. The value $N_R=1.0$ indicates the success of the DFM [30]. Whereas, the deviation of N_R from unity would imply the necessity to perform corrections in the normalization of the effective NN interaction used for each DFM, associated with the different density profiles [30]. The values of N_R applied in the analysis of the density distributions of the ^{14}Be nucleus by ^{12}C have been listed in Table 1. The N_R values used in the analysis of the GO-2n, GO-4n and FG density distributions are unity while the values N_R of

the other density distributions present the deflection from unity. This is important by means of using of the GO-2n, GO-4n and FG density distributions. The DFM calculation with the GO-2n, GO-4n and FG densities can describe the ^{14}Be + ^{12}C quasi elastic scattering data with $N_R=1$. The fit is not perfect for the other models. In these cases the normalization N_R was changed from unity in order to fit the cross-section. We conclude that the GO-2n, GO-4n and FG models without renormalization among the eight density distributions analyzed for the ^{14}Be nucleus showed better results than the ones presented in the literature.

5. SUMMARY AND CONCLUSIONS

In the present study, we have performed the DFM calculations for the quasielastic scattering of the ^{14}Be + ^{12}C system. The eight different density distributions of the ^{14}Be exotic nucleus have been used. It is noticed that the results of the GO-2n, GO-4n and FG density distributions are generally better than the results of the other density distributions. However, we can say that all the ^{14}Be matter density profiles fit to some extend the experimental data. Our fits to the cross-section are in general much better than the ones found in the literature.

In summary, this work provided a comprehensive analysis on the validity of different density distributions of the ^{14}Be nucleus. Our study has shown better fits than previous OM calculations, without the necessity of

surface terms for the real and imaginary parts of the optical potential. Also, this study emphasizes the importance of the internal dynamics of the [14]Be nucleus through the density profiles that take into account the neutron halo.

ACKNOWLEDGEMENT

CONFLICT OF INTEREST

No conflict of interest was declared by the authors.

REFERENCES

[1] Tanihata, I., Hamagaki, H., Hashimoto, O., Shida, Y., Yoshikawa, N., Sugimoto, K., Yamakawa, O., Kobayashi, T., Takahashi, N., "Measurements of interaction cross sections and nuclear radii in the light p-shell region", *Phys. Rev. Lett.*, 55: 2676 (1985).

[2] Hansen, P.G. and Jonson, B., "The neutron halo of extremely neutron-rich nuclei", *Europhys. Lett.*, 4: 409 (1987).

[3] Zhukov, M.V., Danilin, B.V., Fedorov, D.V., Bang, J.M., Thompson, I.J., Vaagen, J.S., "Bound state properties of Borromean halo nuclei: ^{6}He and ^{11}Li", *Phys. Rep.*, 231:151-199 (1993).

[4] Thompson, I.J. and Zhukov, M.V., "Structure and reactions of the ^{12,14}Be nuclei", *Phys. Rev. C*, 53: 708 (1996).

[5] Tanihata, I., "Nuclear radii and change in shell structure: A halo driven new magic number N=16", *Nucl. Phys. A*, 682: 114-123 (2001).

[6] Jonson, B., "Light dripline nuclei", *Phys. Rep.*, 389: 1-59 (2004).

[7] Tanihata, I., Kobayashi, T., Yamakawa, O., Shimoura, S., Ekuni, K., Sugimoto, K., Takahashi, N., Shimoda, T., Sato, H., "Measurement of interaction cross sections using isotope beams of Be and B and isospin dependence of the nuclear radii", *Phys. Lett. B*, 206: 592-596 (1988).

[8] Tanihata, I., "Neutron halo nuclei", *J. Phys. G. Nucl. Part. Phys.*, 22: 157 (1996).

[9] Hansen, P.G., Jensen, A.S., Jonson, B., "Nuclear halos", *Ann. Rev. Nucl. Part. Sci.*, 45: 591-634 (1995).

[10] Ye, Y.L., Pang, D.Y., Zhang, G.L., *et al.*, "Study of the halo nucleus ^{6}He through the direct nuclear reactions", *J. Phys. G. Nucl. Part. Phys.*, 31: S1647-S1653 (2005).

[11] Aygun, M., Boztosun, I., Rusek, K., "Parametrized form of the dynamic polarization potential for the ^{6}He + ^{208}Pb interaction", *Mod. Phys. Lett. A*, 28: 1350112 (2013).

[12] Aygun, M. and Boztosun, I., "An extended analysis of the elastic scattering of ^{6}Li(^{6}He, ^{6}He)^{6}Li system at 17.9 MeV", *Few-Body Syst.*, 55: 203-209 (2014).

[13] Aygun, M., Boztosun, I., Sahin, Y., "A study on the fresnel diffraction of ^{6}He by means of different microscopic density distributions", *Phys. At. Nuc.*, 75: 963-968 (2012).

[14] Aygun, M., "A theoretical study on ^{120}Sn(^{6}He, ^{6}He)^{120}Sn elastic scattering", *Ann. Nucl. Energy*, 51: 1-4 (2013).

[15] Aygun, M., Kucuk, Y., Boztosun, I., Ibraheem, A.A., "Microscopic few-body and gaussian-shaped density distributions for the analysis of the ^{6}He exotic nucleus with different target nuclei", *Nucl. Phys. A*, 848: 245-259 (2010).

[16] Sugimoto, T., Nakamura, T., Kondo, Y., *et al.*, "The first 2^+ state of ^{14}Be" *Phys. Lett. B*, 654: 160-164 (2007).

[17] Suzuki, T., Kanungo, R., Bochkarev, O., *et al.*, "Nuclear radii of ^{17,19}B and ^{14}Be", *Nucl. Phys. A*, 658: 313-326 (1999).

[18] Ozawa, A., Cai, Y.Z., Chen, Z.Q., *et al.*, "Measurements of the interaction cross-sections for ^{14}Be and ^{14,15}B as projectiles with a new scheme at RIBLL", *Nucl. Instr. and Meth. B*, 247: 155-160 (2006).

[19] Aksyutina, Yu., Aumann, T., Boretzky, K., *et al.*, "Study of the ^{14}Be continuum: identification and structure of its second 2^+ state", *Phys. Rev. Lett.*, 111: 242501 (2013).

[20] Labiche, M., Orr, N.A., Marqués, F.M., *et al.*, "Halo Structure of ^{14}Be", *Phys. Rev. Lett.*, 86: 600 (2001).

[21] Al-Khalili, J.S., Tostevin, J.A., Thompson, I.J., "Radii of halo nuclei from cross section measurements", *Phys. Rev. C*, 54: 1843 (1996).

[22] Tarutina, T., Thompson, I.J., Tostevin, J.A., "Study of ^{14}Be with core excitation", *Nucl. Phys. A*, 733: 53-66 (2004).

[23] Ozawa, A., Suzuki, T., Tanihata, I., "Nuclear size and related topics", *Nucl. Phys. A*, 693: 32-62 (2001).

[24] Tanihata, I., Savajols, H., Kanungo, R., "Recent experimental progress in nuclear halo structure studies", *Prog. Part. Nucl. Phys.*, 68: 215-313 (2013).

[25] Alkhazov, G.D., Sarantsev, V.V., "Sensitivity of cross sections for elastic nucleus-nucleus scattering to halo nucleus density distributions", ***Phys. At. Nucl.***, 75: 1544-1549 (2012).

[26] Bush, M.P., Al-Khalili, J.S., Tostevin, J.A., *et al*., "Sensitivity of reaction cross sections to halo nucleus density distributions", ***Phys. Rev. C***, 53: 3009 (1996).

[27] Ilieva, S., Aksouh, F., Alkhazov, G.D., *et al*., "Nuclear-matter density distribution in the neutron-rich nuclei ^{12,14}Be from proton elastic scattering in inverse kinematics", ***Nucl. Phys. A***, 875: 8-28 (2012).

[28] Zahar, M., Belbot, M., Kolata, J.J., *et al*., "Quasielastic scattering of ^{12,14}Be on ^{12}C", ***Phys. Rev. C***, 49: 1540 (1994).

[29] Mermaz, M.C., "Optical model analysis of ^{12}Be and ^{14}Be quasielastic scattering on a ^{12}C target at 56 MeV per nucleon", ***Phys. Rev. C***, 50: 2620 (1994).

[30] Satchler, G.R. and Love, W.G., "Folding model potentials from realistic interactions for heavy-ion scattering", ***Phys. Rep.,*** 55: 183-254 (1979).

[31] Alkhazov, G.D., Dobrovolsky, A.V., Lobodenko, A.A., "Experimental studies of the nuclear spatial structure of neutron-rich He and Liisotopes", ***Phys. At. Nucl.***, 69: 1124-1131 (2006).

[32] El-Azab Farid, M. and Hassanian, M.A., "Density-independent folding analysis of the ^{6,7}Li elastic scattering at intermediate energies", ***Nucl. Phys. A***, 678: 39-75 (2000).

[33] Karakoc, M. and Boztosun, I., "α-α double folding cluster potential description of the ^{12}C + ^{24}Mg system", ***Phys. Rev. C***, 73: 047601 (2006).

[34] Bertsch G., Borysowicz, J., McManus, H., Love, W.G., "Interactions for inelastic scattering derived form realistic potentials", ***Nucl. Phys. A,*** 284: 399-419 (1977).

[35] Thompson, I.J., "Coupled reaction channels calculations in nuclear physics", ***Computer Phys. Rep.***, 7: 167-212 (1988).

[36] Ilieva, S., "*Investigation of the nuclear-matter density distributions of the exotic ^{12}Be, ^{14}Be and ^{8}B nuclei by elastic proton scattering in inverse kinematics*", PhD thesis, Johannes Gutenberg-Universität in Mainz, 2008.

[37] Alkhazov, G.D., Dobrovolsky, A.V., Egelhof, P., *et al*., "Nuclear matter distributions in the ^{6}He and ^{8}He nuclei from differential cross sections for small-angle proton elastic scattering at intermediate energy", ***Nucl. Phys. A***, 712: 269-299 (2002).

[38] Warner, R.E., Patty, R.A., Voyles, P.M., *et al*., "Total reaction and 2n-removal cross sections of 20-60A MeV ^{4,6,8}He, $^{6-9,11}$Li, and ^{10}Be on Si", ***Phys. Rev. C.***, 54: 1700 (1996).

[39] Chaudhur, A.K., "Density distribution of ^{11}Li and proton elastic scattering from ^{9}Li and ^{11}Li", ***Phys. Rev. C***, 49: 1603 (1994).

[40] Rego, R.A., "Closed-form expressions for cross sections of exotic nuclei", ***Nucl. Phys. A***, 581: 119-130 (1995).